Available online at www.sciencedirect.com
ScienceDirect
Journal of Power Sources 174 (2007) 1142–1146
JOURNAL OF POWER SOURCES
www.elsevier.com/locate/jpowsour

Short communication

Electrochemical performance and ^{7}Li NMR studies on an inverse spinel $LiNi_{1/3}Co_{1/3}Mn_{1/3}VO_4$ for Li-ion batteries

George Ting-Kuo Fey [a,*], P. Muralidharan [a], Yung-Da Cho [a], Pai-Ching Chang [b], Hsien-Ming Kao [b]

[a] *Department of Chemical and Materials Engineering, National Central University, Chung-Li 32054, Taiwan, ROC*
[b] *Department of Chemistry, National Central University, Chung-Li 32054, Taiwan, ROC*

Available online 26 June 2007

Abstract

A new inverse spinel $LiNi_{1/3}Co_{1/3}Mn_{1/3}VO_4$ cathode material was synthesized through a citric acid assisted polyethylene glycol (CA:PEG; 3:1, 3:0.5 and 3:0) polymeric method, followed by calcination at 723 K for 5 h in air. The synthesized compound was characterized by TG/DTGA, XRD, FTIR, TEM, and ^{7}Li NMR techniques. TG/DTGA curves showed that the formation of $LiNi_{1/3}Co_{1/3}Mn_{1/3}VO_4$ occurred between 523 and 673 K and the phase pure crystalline formed at 723 K, as also confirmed by XRD analysis which showed that the crystalline phase peaks formed when heated at 723 K for 5 h in air. TEM images revealed that nanosized particles ranged ~170–190 nm. FTIR spectra showed that all organic residues were removed and $LiNi_{1/3}Co_{1/3}Mn_{1/3}VO_4$ formed. The ^{7}Li MAS NMR spectrum of the $LiNi_{1/3}Co_{1/3}Mn_{1/3}VO_4$ sample revealed that the paramagnetic effect is small and small side band manifolds were observed. The galvanostatic cycling study suggests that the cycle stability and capacity retention were enhanced for $LiNi_{1/3}Co_{1/3}Mn_{1/3}VO_4$ prepared with a CA:PEG molar ratio of 3:1 when it was cycled between 2.8 and 4.9 V (versus Li) at a 0.15*C* rate. The electrochemical impedance behavior suggested that a passive layer was formed on the surface of the cathode materials during continuous cycling.

Keywords: Charge–discharge capacity; Inverse spinel; $LiNi_{1/3}Co_{1/3}Mn_{1/3}VO_4$; Lithium-ion batteries

1. Introduction

Current research and development are aimed at the study of lithium-ion inverse spinel cathode materials such as $LiNiVO_4$, as they display a high voltage plateau near ~4.8 V, whereas $LiCoVO_4$ and $LiMnVO_4$ exhibit their plateau near 4.2 and 3.8 V, respectively [1,2]. In general, the theoretical capacity of inverse spinel vanadates possess about 148 mAh g^{-1}, but practically they deliver a low charge–discharge capacity of about ~45–50 mAh g^{-1} accompanied by a large irreversible capacity loss (~40%) and upon continuous cycling, their capacity drops drastically [1,2]. Consequently, in order to improve their capacity and cycle performance, Fey et al. [3–5], Lai et al. [6], Schoonman and co-workers [7,8] and other researcher groups, studied improving electrochemical performance and cycle stability by co-doping various transition metal ions (Ni, Cu, Cr and Fe) with $LiCoVO_4$. Even though wide studies have been carried out on the inverse spinel cathode materials, a better combination of various co-doped ion compositions are needed to stabilize their structure, capacity, cycle stability and irreversible capacity loss. Therefore, we focus our attention on synthesizing a mixed composition of $LiNiVO_4$ by partially substituting Ni^{2+} in the octahedral sites with 1/3rd Co^{2+} and 1/3rd Mn^{2+} ions [9], so as to increase the reversibility of Li-ions (de)intercalate-ion in the active cathode material.

In order to achieve better properties in a material, various preparative methods [1–12] have been used. Park et al. [13] described for the $LiNi_{1/3}Co_{1/3}Mn_{1/3}O_2$ material, that the synthesis process plays an important role in determining the phase pure oxide material. Therefore, an advantageous citric acid assisted with PEG method was followed that facilitates the synthesis of nanosized particles with a larger surface area required for enhancing Li-ion (de)intercalation and also low temperature syntheses. Hence in this work, we have attempted to synthesize a combination of a novel mixed composition and nanoparticulate $LiNi_{1/3}Co_{1/3}Mn_{1/3}VO_4$ through a polymeric citrate assisted with and without PEG method. The structural and electrochemical properties of the prepared materials were char-

* Corresponding author. Tel.: +886 3 425 7325; fax: +886 3 425 7325.
E-mail address: gfey@cc.ncu.edu.tw (G.T.-K. Fey).

0378-7753/$ – see front matter © 2007 Elsevier B.V. All rights reserved.
doi:10.1016/j.jpowsour.2007.06.097

acterized. We also investigated the effect of Mn substitution on the local lithium environments and long-range structures. The ^{7}Li NMR has been shown to be a sensitive probe of the local atomic and electronic environments of Li^+ ions in a variety of electrode materials [14,15]. Therefore, ^{7}Li magic angle spinning (MAS) NMR was used to characterize the structure of $LiNi_{1/3}Co_{1/3}Mn_{1/3}VO_4$, since the ^{7}Li NMR spectra are sensitive to short distance coupling with the paramagnetic transition metal ions.

2. Experiment

The $LiNi_{1/3}Co_{1/3}Mn_{1/3}VO_4$ cathode material was synthesized by a CA:PEG polymeric method, whose molar ratios were varied as 3:1, 3:0.5 and 3:0. Stoichiometric amounts of Li_2CO_3, $NiCO_3{\cdot}2Ni(OH)_2{\cdot}4H_2O$, $Co(CH_3COO)_2{\cdot}4H_2O$, $Mn(NO_3)_2{\cdot}4H_2O$ and NH_4VO_3 (Acros Organics, >98%) were combined to give $LiNi_{1/3}Co_{1/3}Mn_{1/3}VO_4$, through a detailed procedure as described elsewhere [16]. The dried polymeric gel precursor was heated at a ramping rate of 2 K min^{-1} and maintained at 473 K for 3 h, 573 K for 3 h and 723 K for 5 h in air, with intermediate grinding.

The thermal analysis (TG/DTGA) measurement was carried out on a Perkin-Elmer TGA-7 series, at a heating rate of 20 K min^{-1} from 323 to 773 K. An X-ray diffractometer (XRD), Siemens D-5000, Mac Science MXP18, equipped with a nickel-filtered Cu Kα radiation source (λ = 1.5405 Å) between 15° and 80° in steps of 0.05° was used for structural analysis. The microstructures of the particles were examined by a JEOL JEM-200FXII transmission electron microscope (TEM) equipped with a LaB_6 gun. Fourier transform infrared (FTIR) spectra were recorded from 400 to 4000 cm^{-1} on powdered samples using the KBr wafer technique in a Jasco-410 FTIR instrument.

The ^{7}Li MAS NMR was recorded on a Varian Infinityplus-500 NMR spectrometer at 193.73 MHz, with a 4 mm Chemagnetic probe. The samples were mixed with dry MgO (typically 60–70% in weight) in order to facilitate the sample spinning, since they may exhibit metallic or paramagnetic properties. In order to facilitate the phasing of the spinning side bands, a linear prediction method was applied to process the NMR data. Typically, the 90° pulse duration was 3.0 μs, the spinning speed was 14 kHz, the spectral width was in the 100–500 kHz range, and the recycle delay was 1 μs. ^{7}Li Chemical shifts were externally referenced to a 1 M LiCl aqueous solution at 0 ppm.

The electrochemical performances of the cathode were carried out with coin type cells of the 2032 configuration and were assembled in an argon-filled VAC MO40-1 glove box. The cell constituents as described elsewhere [16]. The cells charge–discharge cycles were preformed at a 0.15 C rate between 2.8 and 4.9 V, at 298 K, in a multi-channel battery tester (Maccor 4000). Coin cells fully charged to 4.9 V and also charged at different voltages were subjected to impedance measurements using a Schlumberger 1286 electrochemical interface and frequency response analyzer (Model 1255), driven by Corrware software (Scribner Associates). The frequency range was 65 kHz to 0.001 Hz and the amplitude of the perturbation signal was 20 mV at 298 K.

3. Results and discussion

Fig. 1 shows the TGA/DTGA curves of the $LiNi_{1/3}Co_{1/3}Mn_{1/3}VO_4$ precursor. In Fig. 1, the TGA curve shows a step-wise weight loss in the temperature ranges from 323 to 410 K, 410–629 K, 629–713 K and there was no weight loss after 723 K. The observed initial weight loss of 4% was attributed to the loss of water and unwanted organic residues. In the second temperature range of 410–629 K, the metal complex polymeric network formed between the acid group of citrate and the hydroxyl group of PEG decomposed into intermediates and formed crystalline $LiNi_{1/3}Co_{1/3}Mn_{1/3}VO_4$ compound, which corresponds to the 20% weight loss. In the third temperature range 629–713 K, the intermediates completely decomposed and phase pure $LiNi_{1/3}Co_{1/3}Mn_{1/3}VO_4$ was formed. Most of the combustion process was initiated in this temperature range, as evidenced by the strong DTG peak and the decomposition of the complex polymeric network facilitates the formation of nano-phase compound. In Fig. 1, the weight loss stops at 723 K and hence, all powders were sintered at 723 K for 5 h in air.

Fig. 2 shows the XRD pattern for the $LiNi_{1/3}Co_{1/3}Mn_{1/3}VO_4$ sample heated at 723 K for 5 h in air. From Fig. 2, it is observed that the crystalline single phase compound was obtained when calcined at 723 K for 5 h in air, which belongs to the inverse spinel structure. The increased lattice constant a value and the crystal cell volume for the sample were 8.297 Å and 571.3 Å^3, respectively [1,6] and their increase should be due to the substitution Ni^{2+} and Co^{2+} ions by a large ionic radius of Mn^{2+} ions in the octahedral sites. The TEM micrograph of the $LiNi_{1/3}Co_{1/3}Mn_{1/3}VO_4$ cathode material revealed that the formed crystalline are spherical nanoparticles range from ~170 to 190 nm [16].

Fig. 3a–c shows the FTIR spectra of $LiNi_{1/3}Co_{1/3}Mn_{1/3}VO_4$ heated at 423 K for 24 h, 573 K for 3 h and 723 K for 5 h, respectively. In Fig. 3a and b, the broad band observed in the region 3400–3600 cm^{-1} is due to the presence of stretching modes of OH groups present in the complex network of CA and PEG [17]. The FTIR band observed at 1594 cm^{-1} is due to the asymmetric vibrations of COO^- groups with the metal ions. The

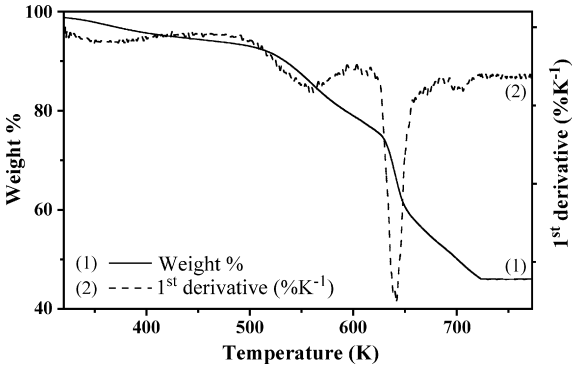

Fig. 1. TGA/DTGA for $LiNi_{1/3}Co_{1/3}Mn_{1/3}VO_4$ prepared by a CA:PEG (3:1) polymeric route.

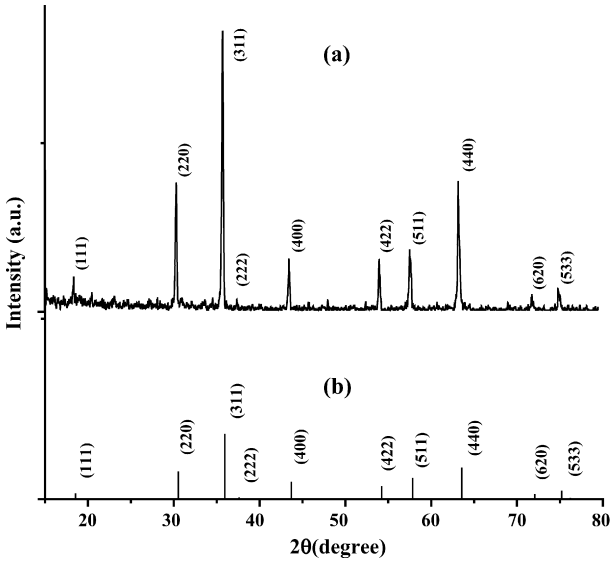

Fig. 2. XRD patterns for (a) $LiNi_{1/3}Co_{1/3}Mn_{1/3}VO_4$ prepared by CA:PEG (3:1) polymeric route and heated at 723 K for 5 h and (b) JCPDS (#38-1935) $LiNiVO_4$.

bands observed at 1074 and 1314 cm^{-1} are due to asymmetric stretching of C–O–C groups in the polymeric network. Thus, the FTIR spectra revealed the heated compounds at 423 K and 573 K were formed of metal carboxylates, thereby, confirming that the citric acid and PEG complex chelates the metal ions. In Fig. 3b, the reduction in the intensity of the bands corresponds to the elimination of organic residues and appearance of new bands corresponding to the formation of crystalline $LiNi_{1/3}Co_{1/3}Mn_{1/3}VO_4$. In Fig. 3c, the CA and PEG complex bands completely disappeared and formed a pure crystalline $LiNi_{1/3}Co_{1/3}Mn_{1/3}VO_4$ compound. The observed results of the FTIR are correlated with TGA curves, which confirmed the decomposition of organic components and the formation of crystalline compound. In Fig. 3c, there is broad strong band in the region 600–915 cm^{-1} that can be assigned to a stretching vibration between the oxygen and V^{5+} ions of the VO_4 tetrahedron in which four types of cations, namely Li, Co, Ni and Mn, may be bonded. The band at 448 cm^{-1} is attributed to symmetrical Li–O stretching [18].

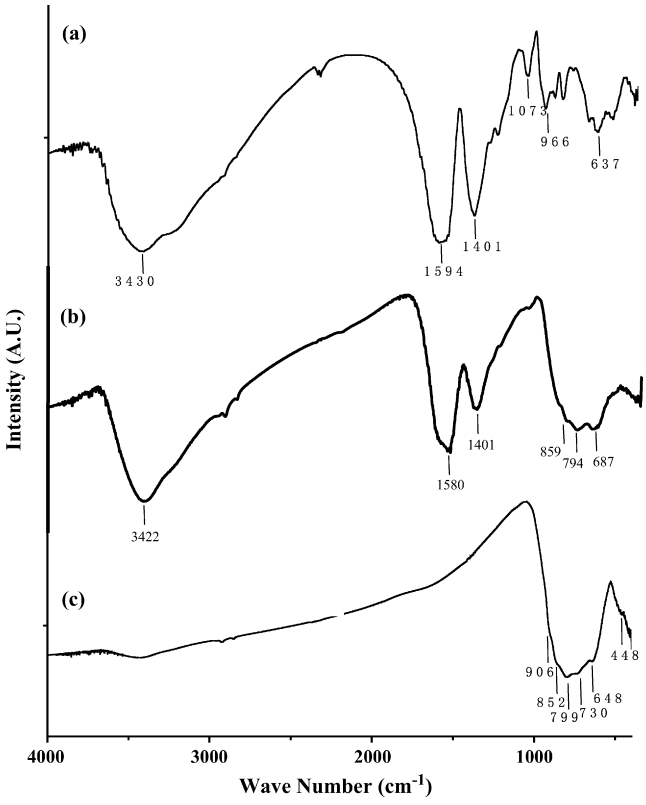

Fig. 3. FTIR spectra for $LiNi_{1/3}Co_{1/3}Mn_{1/3}VO_4$. (a) Heated at 423 K for 24 h. (b) Heated at 573 K for 3 h. (c) Heated at 723 K for 5 h.

Fig. 4 shows the ^7Li MAS NMR spectrum for the $LiNi_{1/3}Co_{1/3}Mn_{1/3}VO_4$ sample, together with that of $LiNi_{1/2}Co_{1/2}VO_4$ for comparison. The spectra are characterized by a single isotropic sharp peak at 0 ppm and spinning sideband manifolds, as expected for paramagnetic materials. This indicates that both materials contain a single type of ^7Li site, and the ^7Li local environments did not significantly change upon Mn substitution. However, much less intense sidebands were observed for $LiNi_{1/3}Co_{1/3}Mn_{1/3}VO_4$, compared to those for $LiNi_{1/2}Co_{1/2}VO_4$. The large spinning sidebands in the ^7Li MAS NMR spectrum of $LiNi_{1/2}Co_{1/2}VO_4$ mainly result from the paramagnetic interaction between the lithium nucleus and transition metal unpaired electrons. The weak intensities of spinning sidebands observed for $LiNi_{1/3}Co_{1/3}Mn_{1/3}VO_4$ indicate that the paramagnetic electron effects in this sample are not important. They may result from lattice expansion upon Mn substitution, which makes the lithium nucleus more distant from the lattice transition metal ions. As a result, the paramagnetic effect is small and small sideband manifolds were observed in the ^7Li MAS NMR spectrum of $LiNi_{1/3}Co_{1/3}Mn_{1/3}VO_4$ cathode material.

Fig. 5 shows the electrochemical performance for the $LiNi_{1/3}Co_{1/3}Mn_{1/3}VO_4$ cathode synthesized with various molar ratios of CA:PEG of 3.0:1.0, 3.0:0.5 and 3.0:0, at 298 K. The initial charge capacities of the $LiNi_{1/3}Co_{1/3}Mn_{1/3}VO_4$ cathode synthesized with the above CA:PEG ratios were

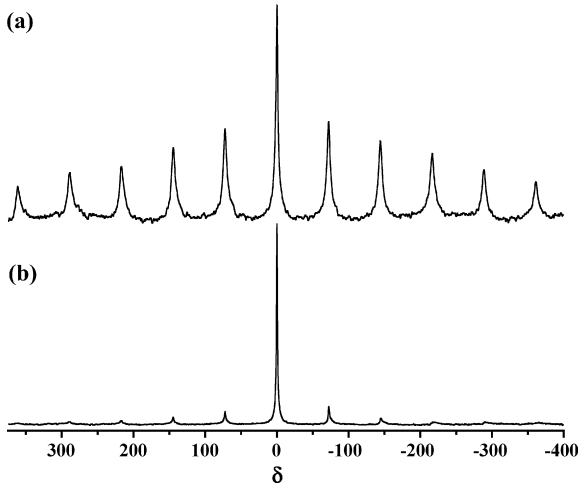

Fig. 4. ^7Li MAS NMR spectra of (a) $LiNi_{1/2}Co_{1/2}VO_4$ and (b) $LiNi_{1/3}Co_{1/3}-Mn_{1/3}VO_4$, acquired at a spinning speed of 14 kHz.

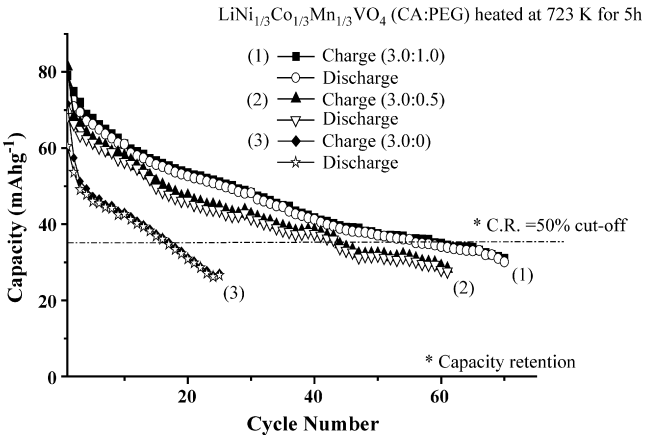

Fig. 5. Cycling behavior of the $LiNi_{1/3}Co_{1/3}Mn_{1/3}VO_4$ cathode material. Charge–discharge: 0.15*C* rate between 2.8 and 4.9 V at 298 K.

79, 68 and 71 mAh g^{-1} and discharge capacities were 70, 66 and 60 mAh g^{-1}, respectively. After 20 cycles, the discharge capacities and coulombic efficiencies were 53, 46 and 31 mAh $g^{-1}$and 76%, 70% and 51%, respectively. In order to compare the effect of various molar ratios of CA:PEG content used in the synthesis process on the cycling performance of Li/$LiNi_{1/3}Co_{1/3}Mn_{1/3}VO_4$ cells, a preset cut-off value of 50% capacity retention was fixed. Based on this cut-off regime, the compounds synthesized with CA:PEG 3:1, 3:0.5 and 3:0 contents could sustain up to 60, 44 and 17 cycles, respectively. From Fig. 5, it is notable that the compound synthesized with CA:PEG content of 3:1 exhibited a smaller initial drop in the discharge capacity 9 mAh g^{-1}.

Table 1 shows a comparison of the first cycle discharge capacity and the irreversible capacity loss for the various co-doped inverse spinel cathodes and from the results, it is concluded that the $LiNi_{1/3}Co_{1/3}Mn_{1/3}VO_4$ compound exhibited a small irreversible capacity loss and an excellent discharge capacity. A possible explanation for the improved capacity retention and cycle stability is the lattice expansion of the Mn-doped cathode material that was established from the ^{7}Li MAS NMR analysis, which is favorable for the Li^+ (de)intercalation process. Thus, the composition of the compound, the co-doped Co and Mn ions substituting for the Ni ions, and the preparation method are suitable for obtaining better discharge capacity and enhanced cycle stability cathode material compared to the literature reported inverse spinel vanadate cathodes [3–6,19].

Fig. 6a and b show the impedance spectra (Z' versus Z'') for $LiNi_{1/3}Co_{1/3}Mn_{1/3}VO_4$ at its first cycle when charged at different cell voltages 4.3, 4.5 and 4.9 V and charged at 4.9 V as function of cycle number, respectively. In Fig. 6a and b, the high frequency semicircle represents the impedance due to a surface film on the oxide electrode and the low-frequency semicircle is related to a slow charge transfer process at the interface, as well as a capacitance at the oxide interface. The Warburg tail implies that the electrode processes under this condition are controlled by diffusion.

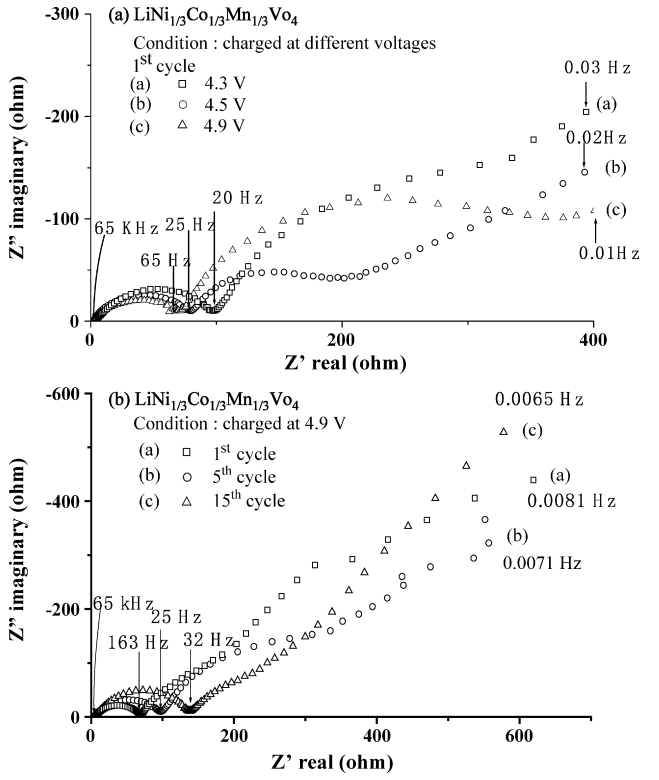

Fig. 6. Electrochemical impedance plots of $LiNi_{1/3}Co_{1/3}Mn_{1/3}VO_4$ sample heated at 723 K for 5 h (a) as a function of different voltages and (b) as a function of cycle number at 298 K.

The electrode kinetics was determined as a function of Li ions deintercalation from the lattices at different voltages during the charge process. In Fig. 6a, it is observed that the cell charged at 4.3, 4.5 and 4.9 V, showed impedance of about 98, 79 and 65 Ω, respectively. Thus, the charge process was accompanied by the deintercalation of Li ions from the crystal lattices and the response changes drastically with a decrease in the cell impedance upon charge to 4.9 V.

From Fig. 6b, it is observed that the solution resistance undergoes very small changes upon cycling from 5.90 to

Table 1
A comparison of the electrochemical performance of the co-doped inverse spinel vanadate cathode materials

Cathode material	First cycle discharge capacity (mAh g^{-1})	Irreversible capacity loss (mAh g^{-1})	Charge–discharge voltage (V)	*c*-rate	Refs.
$LiNi_{0.5}Co_{0.5}VO_4$	44	23	4.5–3.0	0.1	[5]
$LiNi_{1-x}Mn_xVO_4$	30	40	4.8–3.0	0.1	[6]
$LiCo_{0.94}Fe_{0.06}VO_4$	73	27	4.5–3.0	0.1	[7]
$LiNi_{0.5}Co_{0.5}VO_4$	68	25	4.9–2.8	0.15	[19]
$LiNi_{1/3}Co_{1/3}Mn_{1/3}VO_4$	70	9	4.9–2.8	0.15	Present work

7.1 Ω. The small changes in solution resistance are ascribed to the complex chemistry of lithium in electrolyte solutions that result in slight modification in the content of the conducting species in the solution [20]. However, the size of the semicircle increased with cycling. An evaluation of the changes in resistance as a function of cycle number shows that the resistance of the cathode particles increased from 67, 94 and 138 Ω for 1st, 5th and 15th cycles, respectively. The results reveal that during repeated cycling, the surface of $LiNi_{1/3}Co_{1/3}Mn_{1/3}VO_4$ is formed of a passive film of polycarbonates, polymeric hydrocarbons, LiF, Li_xPF_y and $Li_xPF_yO_z$ [21,22] which gets adhered as a thick dense layer, resulting in it becoming a passive layer for the electrochemical reaction. Thus, the constituents of passive film change with the reaction between vanadates cathode electrode and electrolyte, resulting in a decrease in cycle life when charged at high voltages.

4. Conclusions

Pure crystalline $LiNi_{1/3}Co_{1/3}Mn_{1/3}VO_4$ cathode material was successfully prepared by a citric acid assisted PEG polymeric method by varying the PEG content. TGA curves revealed the phase pure crystalline compound occurred at 723 K, a phenomenon also evident from the XRD and FTIR results. The electrochemical measurements of the $LiNi_{1/3}Co_{1/3}Mn_{1/3}VO_4$ synthesized with CA:PEG 3:1 content could sustain up to 60 cycles for coulombic efficiencies of 50% when charged at a high voltage of 4.9 V. The improved capacity retention and cycle stability was due to the lattice expansion of the Mn-doped cathode material that was substantiated through ^{7}Li MAS NMR analysis. Impedance spectra of the cathode suggest that its interaction with the electrolyte during electrochemical cycling, which results in a decrease in cycle efficiency, is due to the resistance offered by the passive layer on the surface of cathode when charged at a high voltage such as 4.9 V.

Acknowledgements

Financial support for this work was provided by the National Science Council of the Republic of China under contract No. NSC 93-2214-E-008-004. PMD thanks the NSC for the award of a post-doctoral fellowship.

References

[1] G.T.K. Fey, W. Li, J.R. Dahn, J. Electrochem. Soc. 141 (1994) 2279.
[2] A.K. Padhi, W.B. Archibald, K.S. Nanjundaswamy, J.B. Goodenough, J. Solid State Chem. 128 (1997) 267.
[3] G.T.K. Fey, W.B. Perng, Mater. Chem. Phys. 47 (1997) 279.
[4] G.T.K. Fey, C.S. Wu, J. Pure Appl. Chem. 69 (1997) 329.
[5] G.T.K. Fey, K.S. Wang, S.M. Yang, J. Power Sources 68 (1997) 159.
[6] Q.Y. Lai, J.Z. Lu, X.B. Su, X.Y. Ji, J. Solid State Chem. 165 (2002) 312.
[7] N. Van Landschoot, E.M. Kelder, P.J. Kooyman, C. Kwakernaak, J. Schoonman, J. Power Sources 138 (2004) 262.
[8] N. Van Landschoot, E.M. Kelder, J. Schoonman, Solid State Ionics 166 (2004) 307.
[9] T. Ohzuku, Y. Makimura, Chem. Lett. (2001) 642.
[10] S.H. Park, K.S. Park, Y.K. Sun, K.S. Nahm, Y.S. Lee, M. Yoshio, Electrochim. Acta 46 (2001) 1215.
[11] C.H. Chen, E.M. Kelder, M.J.G. Jak, J. Schoonman, Solid State Ionics 86–88 (1996) 1301.
[12] C.-H. Lu, W.-C. Lee, S.-J. Liou, G.T.K. Fey, J. Power Sources 81–82 (1999) 696.
[13] S.-H. Park, H.-S. Shin, S.-T. Myung, C.S. Yoon, K. Amine, Y.-K. Sun, Chem. Mater. 17 (2005) 6.
[14] P.P. Chu, D.L. Huang, G.T.K. Fey, J. Power Sources 90 (2000) 95.
[15] M. Arrabito, S. Bodoardo, N. Penazzi, S. Panero, P. Reale, B. Scrosati, Y. Wang, X. Guo, S.G. Greenbaum, J. Power Sources 97–98 (2001) 478.
[16] G.T.K. Fey, P. Muralidharan, C.Z. Lu, Mater. Lett. 60 (2006) 1209.
[17] Y.M. Hon, K.Z. Fung, S.P. Lin, M.H. Hon, J. Solid State Chem. 163 (2002) 231.
[18] C. Julien, M. Massot, C. Perez-Vicente, Mater. Sci. Eng. B 75 (2000) 6.
[19] L.-Q. Mai, W. Chen, Q. Xu, Q.-Y. Zhu, C.-H. Han, W.-L. Guo, Solid State Ionics 161 (2003) 205.
[20] D. Aurbach, A. Schechter, Electrochim. Acta 46 (2001) 2395.
[21] D. Aurbach, B. Markovsky, A. Rodkin, E. Levi, Y.S. Cohen, H.J. Kim, M. Schmidt, Electrochim. Acta 47 (2002) 4291.
[22] K. Edstrom, T. Gustafsson, J.O. Thomas, Electrochim. Acta 50 (2004) 395.